Proceedings of the 11th International Conference on Fluid Flow, Heat and Mass Transfer (FFHMT 2024)
Chestnut Conference Centre - University of Toronto, Toronto, Canada – June 16-18, 2024
Paper No. 078
DOI: 10.11159/ffhmt24.078

Bounded Pressure-Driven Flow of an Incompressible Electrically Conducting Fluid: Porous Medium and Lubrication Applications

Érick Marcelino Miranda[1], Marcos Fabrício de Souza Aleixo Filho[1], Francisco Ricardo Cunha[1]
[1] University of Brasilia, Faculty of Technology, Department of Mechanical Engineering, Fluid Mechanics of Complex Flows Group - VORTEX
Brasilia, Brazil
erick99marcelino@outlook.com; mffilhoaleixo@gmail.com; frcunha@unb.br

Abstract - This work examines the effects of the interaction of a transversal and uniform magnetic field applied to a flow with an electrically conducting and incompressible fluid. This fluid is bounded by two fixed parallel walls in a channel. The bottom wall consists of a porous medium, where the jump of shear stress is given in terms of a suitable relative velocity by a semi-empirical boundary condition proposed by Beavers and Joseph. The formulation of the flow problem is based on the incompressible magnetohydrodynamic governing equations in terms of non-dimensional variables. The relevant physical parameter measuring the relative importance between magnetic and viscous forces is identified as the Hartmann number. The solution of the problem shows the existence of a flow deceleration strongly dependent upon the Hartmann number. In addition, another interesting result is the observed decrease in the magnitude of the longitudinal component of the magnetic flux density as Hartmann number increases. In conclusion, the application of a transverse magnetic field in the flow of an electrically conducting fluid in tiny pores can produce an effective effect like the flow deceleration produced as the porous medium permeability is decreased. Therefore, it seems to be possible to produce such an effect by just monitoring the magnetic field instead of changing the complex microstructure of the porous medium. Finally, the problem of lubrication with an MHD fluid was addressed. Exact solutions were obtained for the velocity and pressure field. Due to the braking effects caused by the Lorentz force, the pressure gradient is reduced and consequently the support force on the bearing is also reduced. Therefore, the MHD effects for this model undermine the lubrication effects of the purely hydrodynamic model.
Keywords**:** Magnetohydrodynamics, Porous Medium, Beavers and Joseph Boundary Condition, Flow Control by External Magnetic Field, Asymptotic solution, Lubrication Problem.

1. Introduction

Magnetohydrodynamics (MHD) studies the interaction between an electrically conducting fluid (non-polar and non-magnetic) and a magnetic field. Flows with MHD effects are a part of fluid mechanics involving these fluids (such as salted water, ionized gases, or liquid metal) and a magnetic field [1]. The industry utilizes this flow type for several purposes, including convection inhibition, mixing, heating, deceleration, and fluid pumping.

The central governing equation in the MHD problem is the modified Navier-Stokes (with the Lorentz force term) and Maxwell equations [2]. Due to these complex equations, the asymptotic method becomes an important analysis tool. We can consider every MHD problem as a combination of hydrodynamic and magnetic effects. Due to the asymptotic method, we fully recover the hydrodynamic case when we set the magnetic effects to zero in an MHD problem. Therefore, to control the intensity of the MHD effects in the problems, one can use parameters arising from the non-dimensionalization process of the resulting equations. This way, critical non-dimensional parameters such as the Hartmann number (H_a) (ratio of Lorentz to viscous forces) and magnetic Reynolds number (ratio of advection to the diffusion of $\boldsymbol{B}$) are extracted. In this context, an example of MHD flow is an electrically conducting fluid flowing bounded by two fixed flat parallel walls with a uniform transverse magnetic field applied. This problem has various applications, such as in the petroleum industry, cooling systems, aerodynamic heating, and fluid droplets [3], [4].

The main scope of this paper is to solve the flow of an electrically conducting fluid in a channel bounded two walls. Note that in one of the applications studied here, one of the walls is porous. The effect of the magnetic field on the curve of pressure gradient versus flow rate is examined at different Hartmann numbers. The deviation from the linear plot for pure hydrodynamic condition (no-MHD flow) is also explored. Additionally, we calculate the velocity and magnetic field induction profiles, and we shall show how the maximum values of these quantities depend on the

Hartmann number. The effective viscosity (η_{eff}) of the flow is also determined as function of H_a. The studies here are important for engineering applications like drag reduction in channel flows with different boundary conditions by controlling the applied magnetic field.

2. Problem Formulation

We are going to study two problems. The first, called a parallel wall problem, is the MHD flow bounded by two fixed parallel walls, and the second concerns a lubrication bearing problem. For the first, the three boundary conditions of the problem were defined. They refer to the no-slip condition at the upper wall. Beaver and Joseph's condition, defined by a semi-empirical method, will be used at the bottom wall (porous medium), and the sliding velocity will be used at the porous interface [5].

The fluid is bounded by two fixed walls with no-slip boundary conditions for the second problem, called the lubrication problem. The bottom wall is parallel to the x-axis, and the upper wall varies linearly with this axis. From then on, we studied these MHD problems, selected the governing equations, made them non-dimensional and solved them. For the two problems, we employed the asymptotic method to split the MHD from the hydrodynamic effect in the governing equations. In parallel to this, however, these problems were also studied in a purely hydrodynamic context. This way, the governing equations were solved, and made non-dimensional. It is essential to point out that due to the high density of calculations, computational assistance was used in solving the equations for the MHD case.

The studied problems involve an electrically conducting Newtonian fluid interacting with a transverse and

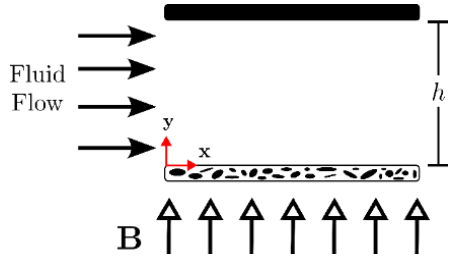

Fig.1: Representation of the proposed problem for the flow between two fixed parallel walls spaced by h. The uniform magnetic field transverse to the applied flow is represented by $\boldsymbol{B}$.

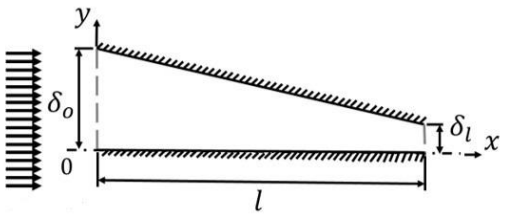

Fig.2: Scheme representing a lubrication bearing with an external magnetic field. The wall distance is $\delta(x)$ and varies from δ_0 until $\delta_l(x)$.

uniform applied magnetic field. A schematic of the proposed problems can be seen in Fig. 1 and Fig. 2. The transverse and uniform magnetic field is denoted as **B**. Note that $\mathbf{B} = \mathrm{B_x(y)}\,\hat{\boldsymbol{e}}_{\boldsymbol{x}} + \mathrm{B_0}\,\hat{\boldsymbol{e}}_{\boldsymbol{y}}$, where B_x is the longitudinal component of the induced magnetic field, and B_0 is the transversal component of the applied field.

Non-dimensionalization simplifies equations by minimizing complexity and reducing the number of variables in the model. Thus, the non-dimensional quantities for the parallel wall problem are given by:

$$y^* = \frac{y}{h}; \quad {v_x}^* = \frac{v_x}{u_m}; \quad p^* = \frac{ph}{\eta u_m}; \quad E_0^* = \frac{E_0}{u_m B_0}; \quad B_x^* = \frac{B_x}{B_0}. \tag{1}$$

And, for the lubrication problem, by: $x^* = \frac{x}{l}$, $\delta^*(x^*) = \frac{\delta(x)}{l}$ and $p^* = \frac{pl}{\eta U}$.

Where the characteristic magnetic flux density, B_0, is given as a characteristic parameter of the problem. The pressure field is denoted by p. The mean velocity is represented as U. The external electric field is E_0. The length of the walls is given by l. The velocity in the x-direction is v_x, and the film velocity in the porous medium is u_m, which flows at a low Reynolds number in a porous medium is calculated by Darcy's law. First, however, we are going to use it to make the

velocity non-dimensional. Furthermore, another essential non-dimensional parameter is the Hartmann number, defined as the ratio between the Lorentz force and the viscous force: $H_a = B_0 h\sqrt{K_e/\eta}$, where K_e and η are the electrical conductivity and viscosity of the fluid, respectively [2]. Another non-dimensional parameter is the Magnetic Reynolds number (ratio between the diffusion time and the advection time of B): $R_{e_m} = hu_m/\nu_m$, where ν_m is the magnetic diffusion coefficient [2]. Note that we used a characteristic length for the definitions of the Hartmann number and the magnetic Reynolds number, which for the parallel wall problem was defined as h. For the lubrication problem, we used the mean velocity as the characteristic velocity in R_{e_m}.

3. Parallel Wall Problem

The configuration shown in Fig.1 describes the problem with MHD effects. The current density is evaluated by the classical Ohm's law as follows [2]:

$$\boldsymbol{J} = K_e(\boldsymbol{E} + \boldsymbol{v} \times \boldsymbol{B}). \tag{2}$$

Using the magnetic field equation and Eq. (2), we obtain the Lorentz force:

$$\boldsymbol{f}_L = \boldsymbol{J} \times \boldsymbol{B} = K_e(E_0 + v_x B_0)\left(-B_0 \hat{\boldsymbol{e}}_{\boldsymbol{x}} + B_x \hat{\boldsymbol{e}}_{\boldsymbol{y}}\right). \tag{3}$$

The governing equation for this problem is $-\nabla p + \eta \nabla^2 \boldsymbol{v} + (\boldsymbol{J} \times \boldsymbol{B}) = 0$. This equation in x and y directions, presented in non-dimensional form, is given by Eq. (4) and Eq. (5), respectively.

$$\sigma^2 + \frac{d^2 v_x^*}{dy^{*2}} - {H_a}^2 {E_0}^* - {H_a}^2 {v_x}^* = 0 \tag{4}$$

$$-\frac{\partial p^*}{\partial y^*} + {H_a}^2 B_x^*(E_0^* + {v_x}^*) = 0 \tag{5}$$

$$\frac{d^2 B_x^*}{dy^{*2}} + R_{e_m} \frac{d{v_x}^*}{dy^*} = 0 \tag{6}$$

With the following boundary conditions: $y^* = 0 \Rightarrow \frac{d{v_x}^*}{dy^*} = \alpha\sigma(u_i - 1)$, $y^* = 1 \Rightarrow {v_x}^*(y^*) = 0$ and ${B_x}^*(y^* = 0) = {B_x}^*(y^* = 1) = 0$, where $\sigma = h/\sqrt{k}$ and the non-dimensional quantity α is called the porosity of the porous medium. Note that, in order to complete the MHD flow formulation, it is necessary to include in the model the equation of magnetic induction transport given by Eq. (6). The analytical solution of the Eq. (4), Eq. (5), and Eq. (6) were obtained using the MATLAB software. This way, the velocity field, magnetic flux density, pressure field, flow rate, and induced electric field were determined.

4. Lubrication Problem

For the lubrication problem, we will not use the asterisk (*) to denote non-dimensional quantities to simplify the notation. By scale analysis, the non-dimensional governing equations of the lubrication problem are:

$$\frac{\partial^2 v_x(y)}{\partial y^2} - {H_a}^2 v_x(y) = \frac{\partial p}{\partial x} + {H_a}^2 \beta; \frac{\partial p}{\partial y} = {H_a}^2 \beta B_x + {H_a}^2 v_x(y) B_x; \tag{7}$$

$$\frac{\partial v_x(y)}{\partial x}+\frac{\partial v_y}{\partial y}=0;\ \frac{\partial v_x(y)}{\partial y}+\frac{1}{R_{e_m}}\frac{\partial^2 B_x}{\partial y^2}=0$$

With the following boundary conditions: $v_x=v_y=0\Rightarrow y=\delta(x)$, $v_x=1\Rightarrow y=0$ and $B_x=0\Rightarrow y=\delta(x)$. The parameter $\beta=\frac{E_o}{B_0U}$ represents the non-dimensional electric field. The solution for the velocity field is:

$$v_x(y)=\mathrm{e}^{H_a\delta}\mathrm{e}^{-H_a\mathrm{y}}\left[\lambda+\frac{\mathrm{e}^{H_a\delta}}{\mathrm{e}^{2H_a\delta}-1}\left(\lambda-\mathrm{e}^{H_a\delta}\lambda+1\right)\right]-\lambda-\frac{e^{H_ay}}{e^{2H_a\delta}-1}\left(\lambda-e^{H_a\delta}\lambda+1\right), \tag{8}$$

where $\lambda=\frac{\beta {H_a}^2-\mathrm{G}}{{H_a}^2}$ and $G=-\frac{\partial p}{\partial x}$. From this result we can obtain the expression for the pressure gradient:

$$G=\frac{2\,{H_a}^2\,\beta+{H_a}^3\,Q_{\mathrm{MHD}}-{H_a}^2\,\mathrm{e}^{H_a\delta}+{H_a}^2+{H_a}^3\,\beta\,\delta-2\,{H_a}^2\,\beta\,\mathrm{e}^{H_a\delta}+{H_a}^2\,Q_{\mathrm{MHD}}\,\mathrm{e}^{H_a\delta}+{H_a}^3\,\beta\,\delta\,\mathrm{e}^{H_a\delta}}{H_a\,\delta-2\,\mathrm{e}^{H_a\delta}+H_a\delta\,\mathrm{e}^{H_a\delta}+2}, \tag{9}$$

where Q_{MHD} is the MHD flow rate and δ is the wall distance which depends on the x.

To observe the MHD effects on the lubrication bearing, the pressure field was resolved considering four Hartmann values, from a very small value ($\mathrm{Ha}=0.01$), which is close to the hydrodynamic case, up to a high Hartmann ($\mathrm{Ha}=2$). From Fig. (6), a decay of the pressure distribution in the x direction is observed with the increase in the Hartmann number. Until $H_a=2$, there is a negative increase in pressure leading to a case alike the positive profile ($\delta_o<\delta_l$), in the pure hydrodynamic case. This leads to the assertion that an intense magnetic field is responsible for a pressure drop in x, weakening the lubrication effect observed in the purely hydrodynamic case. Therefore, the MHD effects for this problem are to inhibit or weaken the support force between bearing and shaft.

5. Asymptotic Solution

Although it is possible to find an exact solution for Eq. (4), an asymptotic analysis of the flow becomes useful for splitting the solution of the problem into two contributions: purely hydrodynamic and correction by magnetic effect. Such methodology has the advantage of splitting the solutions as the sum of the two contributions: hydrodynamic and MHD. Using a regular perturbations method described in [5], [6], the velocity field can be expressed as:

$$v_x^*(y^*)={v_0}^*(y^*)+\varepsilon v_1^*(y^*)+\varepsilon^2 v_2^*(y^*)+\mathcal{O}(\varepsilon^3), \tag{10}$$

where, in this flow problem, the small parameter is $\varepsilon={H_a}^2$. Replacing Eq. (10) in Eq. (4) and after a few algebraic manipulations, we find the following differential equations for different orders of ε:

$$\frac{d^2v_0^*}{dy^{*2}}=-\sigma^2,\mathcal{O}(\varepsilon^0);\ \frac{d^2v_1^*}{dy^{*2}}-{v_0}^*=E_0^*,\mathcal{O}(\varepsilon^1);\ \frac{d^2v_2^*}{dy^{*2}}={v_1}^*,\mathcal{O}(\varepsilon^2) \tag{11}$$

With the following boundary conditions:

$$y^* = 0, \frac{dv_0{}^*(0)}{dy^*} = \alpha\sigma(u_i - 1); \frac{dv_1{}^*(0)}{dy^*} = \frac{dv_2{}^*(0)}{dy^*} = \cdots = 0 \tag{12}$$

$$y^* = 1, v_0{}^* = v_1{}^* = v_2{}^* = \cdots = 0 \tag{13}$$

Finally, we can write the velocity field as:

$$v_x^*(y^*) = v_0{}^*(y^*) + H_a^2 v_1^*(y^*) + \mathcal{O}(H_a^4), \tag{14}$$

Where, $v_0{}^*$ is the solution for the purely hydrodynamic case and $v_1{}^*$ is given by:

$$v_1{}^*(y^*) = \frac{E_0^*}{2}(y^{*2} - 1) + u_i^*\left[\frac{1}{2}(y^{*2} - 1) + \frac{\alpha\sigma}{6}(y^{*3} - 1)\right] + \frac{\alpha\sigma}{6}(1 - y^{*3}) + \frac{\sigma^2}{24}(1 - y^{*4}). \tag{15}$$

If $H_a < 0$, it means that $\varepsilon \ll 0$, so the method gives a highly accurate solution in this regime. As H_a increases, the asymptotic solution diverges from the exact solution of the Eq. (4), as we can verify in Fig. (4). This means that the terms of higher order cannot be neglected in this regime since the Hartmann number is no longer small. Using this asymptotic solution for the velocity field Eq. (14), it is possible to calculate an approximate solution for the magnetic field in the x direction, in which the solution until $\mathcal{O}(H_a^4)$ is expressed by:

$$\begin{aligned} B_x{}^*(y^*) = R_{e_m}&\left[u_i^*\alpha\sigma\frac{(y^* - y^{*2})}{2} + \alpha\sigma\frac{(y^{*2} - y^*)}{2} + \sigma^2\frac{(y^{*3} - y^*)}{6}\right] \\ &+ R_{e_m}H_a^2\left\{E_0^*\frac{(y^* - y^{*3})}{6} + u_i^*\left[\frac{(y^* - y^{*3})}{6} + \alpha\sigma\frac{(y^* - y^{*4})}{24}\right] + \alpha\sigma\frac{(y^{*4} - y^*)}{24}\right. \\ &\left. + \sigma^2\frac{(y^{*5} - y^*)}{120}\right\}, \end{aligned} \tag{16}$$

Note that E_0^* is given by:

$$E_0^* = \left(\frac{H_a^2}{2} + 1\right)^{-1}\left\{\frac{\sigma^2}{3} + \alpha\sigma\frac{(1 - u_i^*)}{2} + H_a^2\left[\frac{\alpha\sigma}{8} + \frac{\sigma^2}{30} - u_i^*\left(\frac{1}{3} + \frac{\alpha\sigma}{8}\right)\right] + \mathcal{O}(H_a^4)\right\}. \tag{17}$$

By Eq. (18), we can determine the flow rate in a purely hydrodynamic contribution and another MHD given by Hartmann orders, as follows:

$$Q^* = \int_0^1 v_0{}^* dy^* + H_a^2 \int_0^1 v_1{}^* dy^* + \mathcal{O}(H_a^4). \tag{18}$$

$$Q^* = \frac{\sigma^2}{12}\frac{(4 + \alpha\sigma)}{(1 + \alpha\sigma)} + \frac{\alpha\sigma}{2(1 + \alpha\sigma)} + H_a^2\left[\frac{-E_0^*}{3} - \sigma^2\frac{(32 + 7\alpha\sigma)}{240(1 + \alpha\sigma)} - \frac{50\alpha\sigma}{240(1 + \alpha\sigma)}\right] + \mathcal{O}(H_a^4), \tag{19}$$

6. Effective Viscosity

Due to the braking effect that the Lorentz force causes in the conducting fluid, it is possible to think of it as a non-ionized fluid but with a higher viscosity responsible for hindering the flow, which is called effective viscosity. The

effective viscosity represents the viscosity that a non-conducting fluid would have in order to present the same relationship between flow rate and pressure gradient as the conducting fluid for a certain Hartmann number, so the viscosity naturally must depend on H_a. In this way, it is possible to express a purely hydrodynamic flow rate, even for an ionized fluid with an equivalent viscosity in the following form [7]:

$$Q = \frac{Gh^3}{12\eta_{eff}}\left[\frac{\alpha\sigma + 4 + 6\alpha/\sigma}{(1+\alpha\sigma)}\right], \tag{20}$$

where η_{eff} is the effective viscosity given, in this flow, by:

$$\eta_{eff} = \eta\left[\frac{6+H_a^2}{3(2+H_a^2)} - H_a^2\frac{(32+7\alpha\sigma+50\alpha/\sigma)}{(\alpha\sigma+4+6\alpha/\sigma)} + \mathcal{O}(H_a^4)\right]^{-1}. \tag{21}$$

7. Results and Discussion

Fig. (3) shows plots of the non-dimensional velocity profile as a function of y for different Hartmann numbers. As the Hartmann number increases, we observe a deceleration of the flow. Additionally, we emphasize that when the

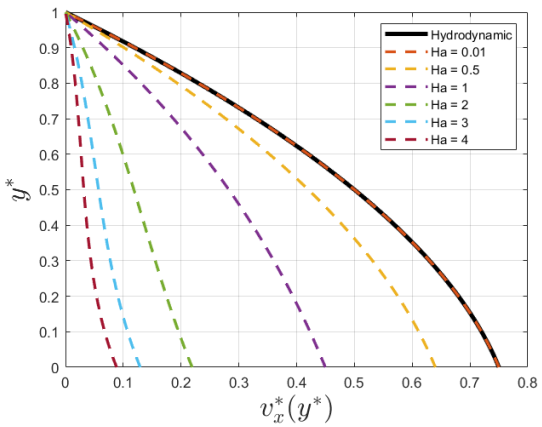

Fig. 3: Non-dimensional flow velocity profiles. The – represents the velocity profile for a hydrodynamic flow. The --- represents the velocity profile for flow with MHD effects about different Hartmann numbers (differentiated by color). $\alpha = 1$, $\sigma = 1$, $\eta = 1$.

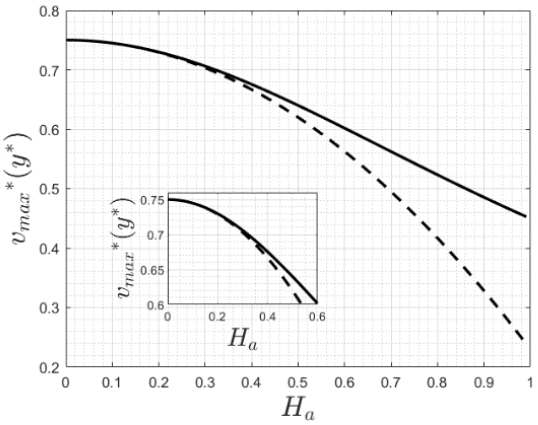

Fig. 4: Comparison between the analytical and asymptotic solution for the maximum velocity profile for a Hartmann number variation from 0 to 1. $\alpha = 1$, $\sigma = 1$, $y^* = 0$. Note that - represents the analytical solution, and --- is the asymptotic solution.

Hartmann number approaches zero, the MHD flow reverts to the purely hydrodynamic flow (H_a = 0). We can see this convergence in Fig. (3), when the velocity profiles for H_a = 0.01 and the hydrodynamic flow overlap. Fig. (4) shows that the maximum velocity occurs in $y^* = 0$ (i.e., bottom wall) because of the sliding condition. Fig. (4) depicts that this maximum velocity decreases when the Hartmann number increases.

Numerous researchers have investigated the magnetic effects on various flows, significantly contributing to our understanding of the phenomenon. For example, studies by [8] demonstrate that magnetic effects decrease flow velocity. Consequently, as the Hartmann number increases, we can expect a reduction in flow rate for the flow analysed in the problem.

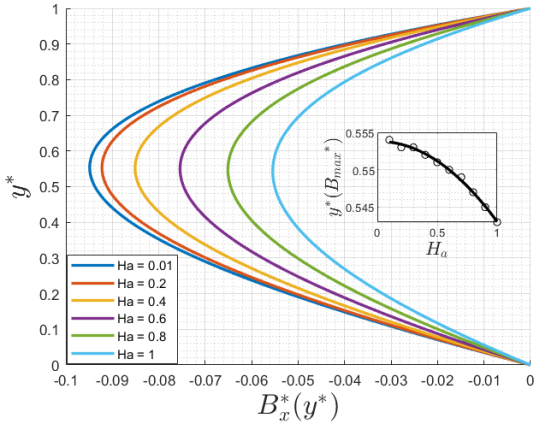

Fig. 5: Profiles of the non-dimensional magnetic field induction in the longitudinal direction. Different colors represent the profiles for the flow with several

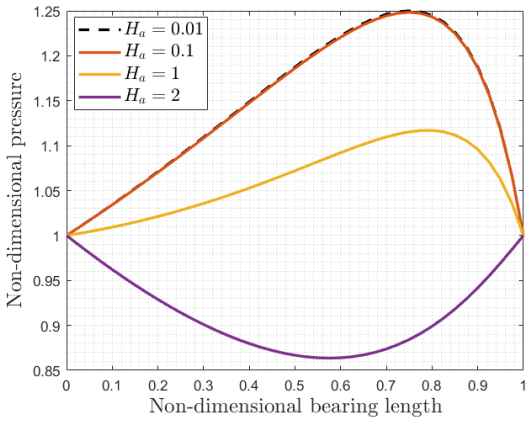

Fig. 6: Pressure profiles between bearing and shaft according to the geometry in que $\delta_o > \delta_l$, for different Hartmann values.

From Fig. (5), the intrinsic coupling between the induced magnetic flux density and the velocity can be seen. As Hartmann is increased, the effects of the Lorentz force slow down the flow, making the modulus of the magnetic flux density smaller.

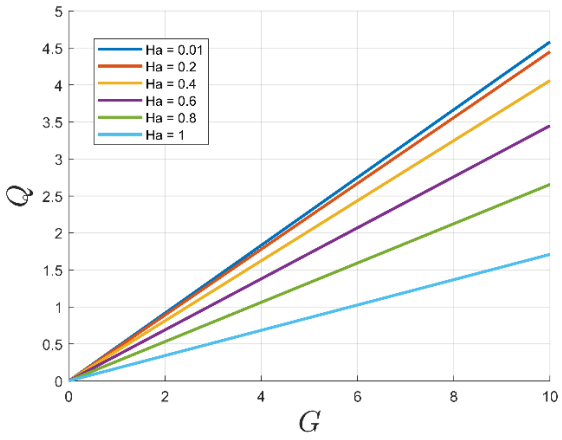

Fig. 7: Flow rate profiles concerning G. Different colors represent the magnetic field induction for the flow with several H_a numbers. $h = 1, \alpha = 1, \sigma = 1$.

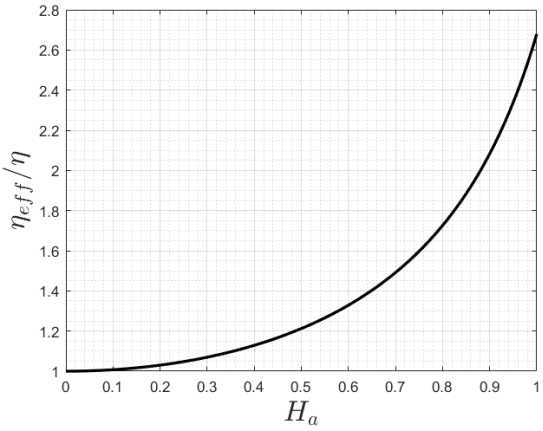

Fig. 8: Non-dimensional effective viscosity as a function of Hartmann number. $\alpha = 1, \sigma = 1$.

Fig. (7) shows the relation between the flow rate and the gradient pressure. If the Lorentz force effect is strong, the flow rate diminishes. Despite this flow rate reduction, the relationship between this magnitude and the pressure gradient remains linear in this Hartmann regime. Plotting the relation in Eq. (21), it is possible to verify by analysing

Fig. (8) that the effective viscosity increases with the Hartmann number as if the MHD effect made the fluid more viscous. Because of this effect, the flow rate decays with the increase of Hartmann, as seen in Fig. (7).

8. Conclusion

In this work, the results have demonstrated how the effects of the MHD Lorentz force can modify the motion of an electrically conducting fluid undergoing a pressure gradient. The magnetic effect can decelerate or accelerate (in this case, control of the intensity of the electric field is always required) the flow, depending on the intensities of magnetic and electrical fields on the conductor fluid.

With the solution of the parallel walls problem, it was possible to obtain the expected results since the velocity profile proved to be coherent with the boundary conditions and the assumptions made. The boundary condition of the porous medium (bottom wall) modifies the velocity profile by accelerating it locally.

The flow problem explored in this paper was similar to the one which occurs in the tiny pores of natural reservoir during oil extraction by a pressure-driven flow. In conclusion, the application of a transverse magnetic field in the flow of an electrically conducting fluid in tiny pores can produce an effective effect like the flow deceleration produced as the porous medium permeability is decreased. Therefore, it seems to be possible to produce such an effect by just monitoring the magnetic field instead of changing the complex microstructure of the porous medium.

Finally, the use of a conductive fluid subject to a magnetic field in a lubrication problem does not help with the lift effect, but rather the opposite, inhibiting or reducing this phenomenon. And the main cause of this is the fact that there is a dampening of the flow caused by the action of the Lorentz force.

Acknowledgements

The authors would like to thank the Brazilian Coordination of Superior Level Staff Improvement (CAPES) for the financial support throughout the development of this work.

References

[1] L. Bühler, “Instabilities in quasi-two-dimensional magnetohydrodynamic flows,” *J Fluid Mech*, vol. 326, pp. 125–150, Nov.1996, doi: 10.1017/S0022112096008269.

[2] P. A. Davidson, *Introduction to Magnetohydrodynamics*, Dec. 2016, doi: 10.1017/9781316672853.

[3] S. Ganesh and R. Delhi Babu, “Steady MHD flow between two parallel porous plates with an angular velocity,” *International Journal of Ambient Energy*, vol. 42, no. 13, pp. 1529–1537, 2021, doi: 10.1080/01430750.2019.1611647.

[4] P. Chandrasekar, S. Ganesh, A. M. Ismail, and V. W. J. Anand, “Magnetohydrodynamic flow of viscous fluid between two parallel porous plates with bottom injection and top suction subjected to an inclined magnetic field,” AIP Conf Proc, vol. 2112, no. 1, Jun. 2019, doi: 10.1063/1.5112329/1024198.

[5] E. J. Hinch, *Perturbation Methods*, Oct. 1991, doi: 10.1017/CBO9781139172189.

[6] J. D. Logan, *Applied Mathematics*, 4th ed. Hoboken, NJ: Wiley-Interscience, May 2013. ISBN: 978-1-118-47580-5.

[7] L. I. A. da Silva, "Incompressible magnetohydrodynamics of conducting fluids in laminar internal flows," Final Year Project, Dept. of Mechanical Engineering, University of Brasilia, Brazil, 2022.

[8] A. Yasmin, K. Ali, and M. Ashraf, “Study of Heat and Mass Transfer in MHD Flow of Micropolar Fluid over a Curved Stretching Sheet,” *Scientific Reports 2020 10:1*, vol. 10, no. 1, pp. 1–11, Mar. 2020, doi: 10.1038/s41598-02061439-8.